Nonradical Mechanism for Methane Hydroxylation by Iron-Oxo Complexes

KAZUNARI YOSHIZAWA*

Institute for Materials Chemistry and Engineering, Kyushu University, Fukuoka 812-8581, Japan

Received November 8, 2005

ABSTRACT

A nonradical mechanism for methane hydroxylation by the bare FeO^+ complex, Fe-ZSM-5 zeolite, and soluble methane monooxygenase is proposed from quantum chemical calculations. This mechanism is applicable when a metal-oxo species is coordinatively unsaturated. Direct interaction between methane and a metal active center can form a weakly bound methane complex in the initial stages of this reaction. Subsequent C−H bond cleavage to form an intermediate with an HO−Fe−CH_3 moiety in a nonradical manner and recombination of the resultant OH and CH_3 ligands take place at a metal active center to form a final methanol complex. Thus, this is a nonradical, two-step reaction. The fact that methyl radical is 10−20 kcal/mol less stable than secondary and tertiary carbon radicals and benzyl radicals leads us to propose this mechanism.

Introduction

The selective oxidation of alkanes[1−5] has attracted increased attention in recent years because of its scientific interest and industrial importance. The direct conversion of methane to methanol is catalyzed by soluble methane monooxygenase (sMMO)[6] under physiological conditions (eq 1), the bare FeO^+ complex[7] in the gas phase, and Fe-ZSM-5 zeolite.[8] The latter two reactions are very similar in that nitrous oxide is used as an oxidant while sMMO uses molecular oxygen. Iron-oxo species are involved in these difficult chemical processes. To develop a man-made catalytic system to realize this fascinating reaction, it is important to reveal the mechanism of the direct process by these catalytic systems.

$$CH_4 + 1/2\ O_2 \rightarrow CH_3OH\ (\Delta H_0 = -30.7\ \text{kcal/mol}) \quad (1)$$

Quantum chemical calculations play a key role in understanding the mechanism of C−H activation, which is an essential, initial process in alkane oxidation, but not well understood because of its extremely rapid reaction rate. Figure 1 shows computed C−H bond energies of alkanes from density functional theory (DFT) calculations. The C−H bond energies at the primary (1°), secondary (2°), and tertiary (3°) carbon atoms of alkanes are approximately 97, 94, and 90 kcal/mol while those at the benzylic positions are less than 85 kcal/mol. Only methane has a C−H bond energy of over 100 kcal/mol among alkanes. The C−H bond energies have a good correlation with computed HOMO−LUMO energy gaps. The fragment molecular orbital (FMO) diagram in Figure 2 tells us how the MOs of tetrahedral CH_4 are formed.[9] The a_1 and t_2

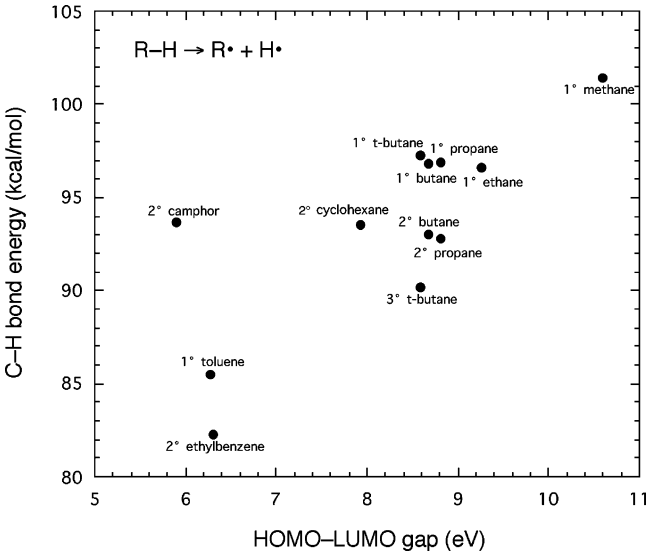

FIGURE 1. C—H bond energies vs. HOMO−LUMO gaps of small alkanes at the B3LYP/6-311++G** level of density functional theory.

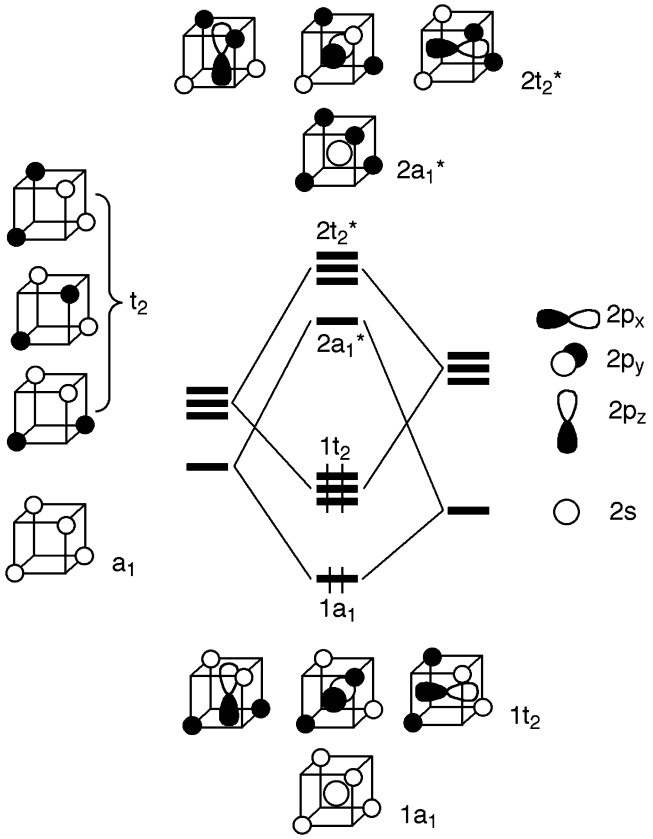

FIGURE 2. Fragment molecular orbital analysis of methane.

Kazunari Yoshizawa received his bachelor's, master's, and Ph. D. degrees at Kyoto University under the direction of Profs. Kenichi Fukui and Tokio Yamabe. After spending one year (1994−1995) at Cornell University as a postdoctoral associate with Prof. Roald Hoffmann, he joined the faculty of Kyoto University, where he became Assistant and then Associate Professor. He moved to Kyushu University as Professor in 2001. His research interests include biochemical reactions and electronic properties of molecules and solids.

* E-mail: kazunari@ms.ifoc.kyushu-u.ac.jp. Fax: 81-92-642-2735.

10.1021/ar050194t CCC: $33.50 © 2006 American Chemical Society
Published on Web 04/14/2006

Scheme 1

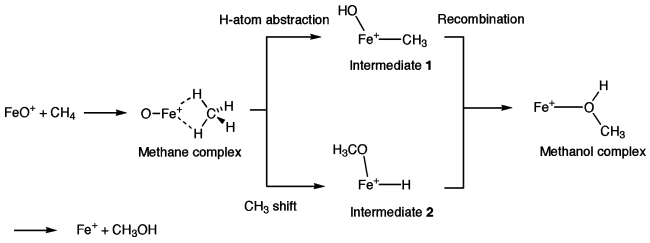

orbitals of the cubic H_4 fragment combine in-phase (out-of-phase) with the s, p_x, p_y, and p_z atomic orbitals of the central carbon atom to form MOs $1a_1$ and $1t_2$ ($2a_1$ and $2t_2$), respectively. The eight-electron CH_4 molecule is very stable in the tetrahedral structure, due to the occupation of the low-lying $1a_1$ and 3-fold degenerate $1t_2$ MOs. The $1t_2$ HOMO and $2a_1$ LUMO have remarkable bonding and antibonding natures with respect to the C−H bonds, respectively, its HOMO−LUMO gap being 10.6 eV at the B3LYP level of DFT. Thus, methane is a very hard molecule, and its C−H activation is difficult.

Alkane hydroxylation is believed to occur by a mechanism involving H-atom abstraction from alkane (R−H) followed by rapid transfer of a metal-bound hydroxyl radical to an intermediate alkyl radical (R•).[10] We have considered whether such a radical mechanism is applicable to methane hydroxylation because methyl radical is 10−20 kcal/mol less stable than secondary and tertiary carbon radicals and benzyl radicals, as seen in Figure 1. This is an important fact that leads us to propose a nonradical mechanism, in which methyl radical is trapped at the iron site. The focus and scope of this manuscript is to look at how the iron active species play a role in the direct conversion of methane to methanol. We now summarize fundamental aspects of methane hydroxylation by FeO^+, Fe-ZSM-5 zeolite, and sMMO, emphasizing our mechanistic studies based on quantum chemical calculations.

Methane Hydroxylation by FeO^+. Gas-phase reactions between the transition-metal-oxide ions (MO^+s) and hydrocarbons are of particular interest since they can be viewed as model reactions for various oxidation reactions by catalytic and enzymatic systems. Methane hydroxylation by MO^+s in the gas phase under ion-cyclotron-resonance conditions has been investigated by Schwarz and co-workers[3,7] and Armentrout and co-workers.[11] There are two possible reaction pathways for methane hydroxylation, as indicated in Scheme 1.[12]

Direct or indirect observations have been made to support the intermediacy of alkane complexes in C−H activation,[13] but their direct observation requires ultrafast spectroscopic techniques at low temperature. The initially formed methane complex $FeO^+(CH_4)$, which takes an η^2-CH_4 coordination, is transformed into intermediates **1** ($HO-Fe^+-CH_3$) and **2** ($H-Fe^+-OCH_3$) by an H-atom abstraction and methyl shift, respectively. The reaction pathway via **1** is energetically more favorable than the other one via **2**.[12a] This result is fully consistent with the prediction of Schwarz and co-workers[7] that **1** plays a central role in the gas-phase reaction between FeO^+ and methane. Intermediate **1** is then transformed into the methanol complex as a result of the recombination of the OH and CH_3 ligands at the metal center.

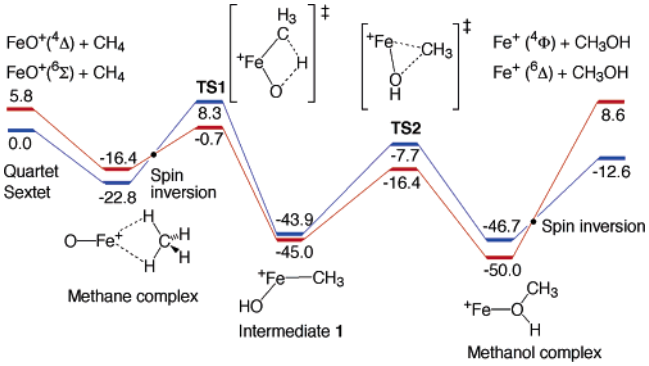

FIGURE 3. Energy diagrams for the reaction $FeO^+ + CH_4 \rightarrow + CH_3OH$ in the sextet and quartet states at the B3LYP/6-311G** level of theory. Relative energies are in kcal/mol.

We show in Figure 3 computed potential energy diagrams in the sextet and quartet states along the reaction pathway.[12b] The initial methane complex is significantly deformed from the T_d-type structure, the H−C−H angle of the coordination side being deformed from 109.5° to 120°. The interactions between the HOMO of the coordinated methane (C−H bonding) and the unfilled orbitals of FeO^+ and between the LUMO of the methane (C−H antibonding) and the filled orbitals of FeO^+ play an essential role in the formation of this complex. One of the hydrogen atoms in the coordinated methane shifts to the oxygen atom via a four-centered transition state (**TS1**), giving rise to intermediate **1**. In the second half of the reaction, a recombination occurs to form a C−O bond via a three-centered transition state (**TS2**), leading to the methanol complex, $Fe^+(CH_3OH)$. This process occurs at a coordinatively unsaturated metal active center, so no radical species is involved in the present mechanism.

We see in Figure 3 two important crossing points between the sextet and quartet potential energy surfaces near the methane complex and the methanol complex. Intrinsic reaction coordinate (IRC) analyses showed that the reaction pathway should involve three crossing seams between the two potential energy surfaces.[14] The first crossing seam is located near **TS1**, and the second and third ones are located in the vicinity of the intermediate and the exit channel, respectively. The spin-forbidden transition in the initial stages of the reaction leads to a significant decrease in the barrier height of **TS1**. To evaluate the spin-forbidden transition in the reaction pathway, we calculated the spin−orbit coupling (SOC) matrix elements along the IRC of the reaction.[15] The strength of SOC between the sextet and the low-lying quartet states is 133.6 cm^{-1} in the methane complex $FeO^+(CH_4)$, 21.4 cm^{-1} in the intermediate $HO-Fe^+-CH_3$, and 0.3 cm^{-1} in the methanol complex $Fe^+(CH_3OH)$. As a result of the spin inversion in the vicinity of **TS1**, the H-atom abstraction step lies slightly below the dissociation limit in the ground sextet state, as shown in Figure 3. Thus,

Table 1. Computed Bond Dissociation Energies (BDE), Atomic Spin Densities for the MO^+ Complexes, and Overall Heats of Reaction (ΔE) for $MO^+ + CH_4 \rightarrow M^+ + CH_3OH$ at the B3LYP/6-311G Level of DFT**

			atomic spin density		
MO^+	state	BDE (kcal/mol)	M	O	ΔE (kcal/mol)
ScO^{2+}	$^1\Sigma^+$	156.1	0.00	0.00	73.5
TiO^+	$^2\Delta$	155.1	1.14	−0.14	72.4
VO^+	$^3\Sigma^-$	137.2	2.33	−0.33	54.5
CrO^+	$^4\Sigma^-$	81.3	3.65	−0.65	−1.3
MnO^+	$^5\Sigma^+$	56.4	4.75	−0.75	−26.2
FeO^+	$^6\Sigma^+$	75.2	3.86	1.14	−12.6
	$^4\Delta$	69.4	3.62	−0.63	–
CoO^+	$^5\Delta$	73.3	2.68	1.32	−25.6
	$^3\Pi$	49.9	2.61	−0.61	–
NiO^+	$^4\Sigma^-$	69.3	1.53	1.47	−26.5
	$^2\Sigma^-$	57.9	−0.23	1.23	–
CuO^+	$^3\Pi$	37.6	0.47	1.47	−50.0
	$^1\Sigma^+$		0.00	0.00	–

Scheme 2

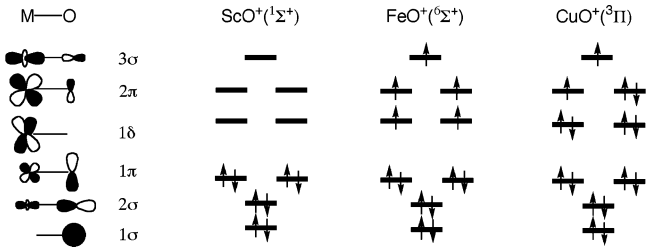

this reaction occurs in the gas phase under adiabatic conditions. This is a good example of the two-state-reactivity mechanism proposed by Shaik and co-workers.[16]

Reactivity of Early and Late MO^+ Complexes. Late transition-metal oxides mediate alkane hydroxylation more effectively than early transition-metal oxides in general. In this section let us consider how late MO^+s perform C−H activation by looking at their simple molecular orbitals. Computed M−O bond dissociation energies, spin densities on the metal and oxygen atoms, and overall heats of reaction for methane hydroxylation listed in Table 1 are in line with the general tendency of the oxidation ability of transition-metal oxides.[17] With an increase in the number of d-electrons, computed bond dissociation energies and overall heats of reaction significantly decrease. Note that the heats of reaction are negative in the late MO^+ complexes, so this reaction is energetically preferred after CrO^+.

The molecular orbitals of MO^+ in Scheme 2 can be partitioned into bonding (2σ and 1π), nonbonding (1σ and 1δ), and antibonding (2π and 3σ) block orbitals. The ScO^+, FeO^+, and CuO^+ complexes can be formally viewed as d^0, $d,^5$ and d^8 complexes, respectively. In the ground state of ScO^+, four pairs of electrons occupy the nonbonding 1σ orbital and the three bonding orbitals to form a strong triple bond just like dinitrogen.[18] The electronic features of TiO^+ and VO^+ are similar to that of ScO^+ because the partially filled nonbonding 1δ set has no direct effect on the metal−oxygen bonds while the three bonding orbitals are fully occupied. These early MO^+ complexes have a very strong triple bond, and accordingly the reactivity of these complexes toward alkanes is low. Since in the high-spin ground states of FeO^+, CoO^+, and NiO^+ all the bonding orbitals are doubly occupied and each 2π orbital is singly occupied, they may resemble triplet dioxygen in the electronic configurations.[18] In contrast to the early MO^+ complexes, the FeO^+, CoO^+, NiO^+, and CuO^+ complexes have low-spin states that are energetically close to the high-spin ground states.

The nonradical mechanism is in good agreement with the reactivity of MnO^+, FeO^+, CoO^+, and NiO^+ and their methanol branching ratios.[3a] For example, MnO^+ has a high reaction efficiency of 40% to methane, but unfortunately the methanol-branching ratio is low (<1%). On the other hand, the reaction efficiency of CoO^+ is low (0.5%), but its methanol-branching ratio is 100%. In the reaction between FeO^+ and methane, the reaction efficiency is 20% and the methanol-branching ratio is 41%. NiO^+ has a high reaction efficiency of 20% and a high methanol-branching ratio of 100%. The selectivity of the reaction by these MO^+ complexes can be explained by the heights of **TS1** for the H-atom abstraction and **TS2** for the recombination.[12b,17] One can expect from Figure 1 that the activation energy from $OMn^+(CH_4)$ to $HO-Mn^+-CH_3$ via **TS1** should be small, but that from $HO-Mn^+-CH_3$ to $Mn^+(CH_3OH)$ via **TS2** should be large. In contrast, the activation energy from $CoO^+(CH_4)$ to $HO-Co^+-CH_3$ should be large, but that from $HO-Co^+-CH_3$ to $Co^+(CH_3OH)$ should be small. Moreover, the activation energy from $NiO^+(CH_4)$ to $HO-Ni^+-CH_3$ should be small, and that from $HO-Ni^+-CH_3$ to $Ni^+(CH_3OH)$ should be small. In fact, our DFT results are fully consistent with this qualitative consideration. [17]

Methane hydroxylation over Fe-ZSM-5 Zeolite. Zeolites that act as micro- or mesoporous hosts for metal oxides mediate lots of catalytic reactions.[19] ZSM-5 zeolite exhibits an extremely high catalytic selectivity for the oxidation of benzene to phenol. Panov and collaborators[20] have suggested that the high reactivity of ZSM-5 zeolite should be ascribed to impurity iron, which is added with starting ingredients at the step of zeolite synthesis. A surface oxygen species called α-oxygen, which is generated on Fe-ZSM-5 zeolite under N_2O decomposition, is proposed to be responsible for the formation of phenol from benzene. The conversion of methane to methanol also takes place over Fe-ZSM-5 zeolite using N_2O as a source of oxygen in 80% yield.[8b,c]

The most difficult problem in considering the mechanism is that no information is obtained about the structure of the active species on Fe-ZSM-5 zeolite. Taking the general features of zeolite into account, we set up a working hypothesis that α-oxygen has relevance to an iron-oxo species supported at the AlO_4 surface site of ZSM-5 zeolite.[21] The activation energy for the decomposition of N_2O at this site was computed to be 2.4 kcal/mol with a cluster model and its formation 63.5 kcal/mol exothermic at the B3LYP level of theory.[21a] We thus expect the decomposition of N_2O to occur at the active site of Fe-ZSM-5 zeolite under experimental conditions. The decomposition of N_2O at the hydrated and dehydrated mononuclear iron sites is recently reevaluated by detailed DFT calculations.[22]

Scheme 3

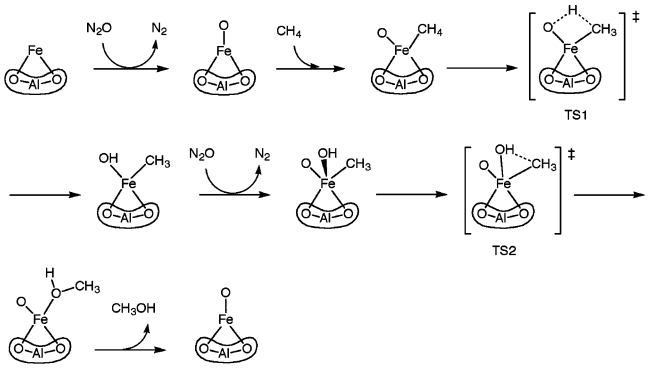

Our mechanistic proposals for methane hydroxylation over Fe-ZSM-5 zeolite are summarized in Scheme 3. The mechanism is essentially identical to that of the gas-phase reaction by FeO^+.[21b] The first step of this reaction is the formation of a methane complex at the coordinatively unsaturated iron site. The Fe ion is closer to one pair of H atoms of the bound methane; this initially formed species is also an η^2-CH_4 complex. Then one of the H atoms of the methane molecule is abstracted via **TS1**, leading to a reaction intermediate that involves resultant OH and CH_3 ligands. The second half of the reaction starts from the intermediate, which is then converted into a methanol complex via **TS2**, in which an Fe−C bond cleavage and a C−O bond formation occur simultaneously.

The methanol complex and the final complex from which methanol is released involve an Fe^I species, which should be reoxidized back to Fe^{III} upon decomposition of N_2O. However, Since Fe^I is a rather unstable oxidation state for iron in general,[21b] Panov and co-workers[8c] proposed a diiron model that reasonably allows the two-electron oxidation and reduction between $Fe^{III}Fe^{III}$ and $Fe^{II}Fe^{II}$. Although we can extend our mechanism to a diiron complex, the formation of the unfavorable Fe^I species is avoidable on the mononuclear model by considering the decomposition of nitrous oxide on an intermediate, as shown in Scheme 3, when the concentration of N_2O is sufficiently high.[23]

Once methanol is produced, further oxidation reactions of methanol into formaldehyde, formic acid, and carbon dioxide can take place more easily than the oxidation from methane to methanol. In the overoxidation processes, there are lots of reaction branches that are comparable in energy. Although many complicated reactions are involved in the metal-mediated combustion, the elementary processes are C−H and O−H cleavage reactions by oxo and hydroxo ligands as well as OH group migrations. As summarized in Figure 4, we proposed possible reaction pathways for the overoxidation processes of methanol to carbon dioxide.[24,25]

Enzymatic Methane Hydroxylation. Methane monooxygenase (MMO) catalyzes the transformation of methane and dioxygen into methanol and water at ambient pressure and temperature.[6] MMO is the first enzyme in the metabolic pathway of methanotrophic bacteria that

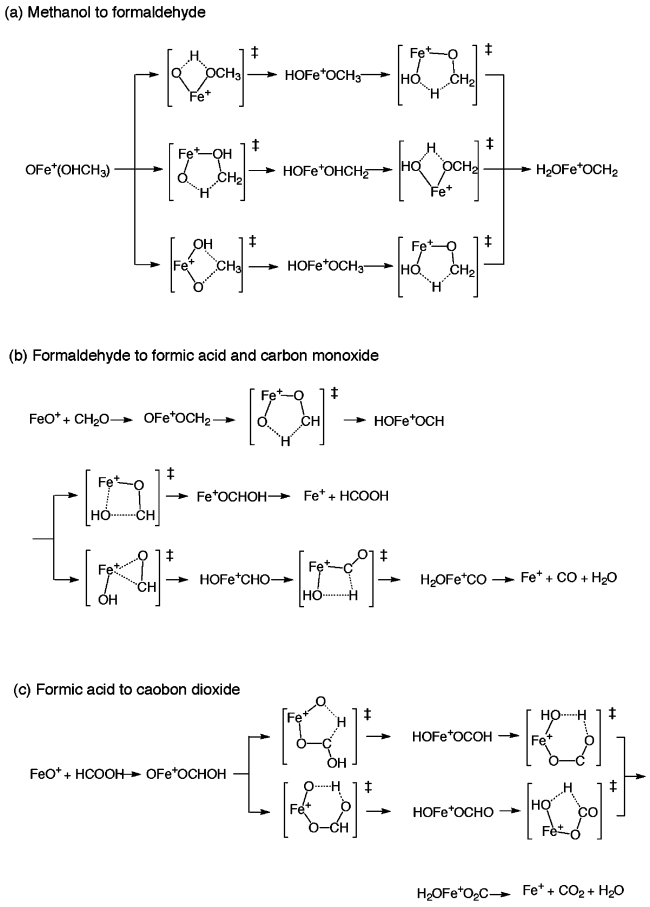

FIGURE 4. Possible mechanisms for the oxidation of methanol to carbon dioxide.

use methane as their sole source of carbon and energy. The two iron atoms at the active site of MMO hydroxylase (MMOH) have octahedral environments in the resting state with the oxidation state of $Fe^{III}Fe^{III}$ (**MMOH**$_{ox}$).[26] Upon reduction of the diiron^{III} state, a carboxylate shift of Glu243 occurs at the active center of the reduced diiron^{II} enzyme to render the iron atoms unsaturated five-coordinate (**MMOH**$_{red}$). Then, dioxygen is bound to the vacant coordination site of the diiron active center. Calculations at various levels of theory demonstrated that the end-on bridging mode into the diiron active site is energetically more stable than the side-on bridging mode.[27] The resultant peroxo intermediate (**MMOH**$_P$) is subsequently converted to the high-valent $Fe^{IV}Fe^{IV}$ intermediate (**MMOH**$_Q$), which has direct reactivity toward methane. From a combined Mössbauer-EXAFS investigation, Que, Lipscomb, and co-workers[28] showed that the active site of **MMOH**$_Q$ should involve a bis(μ-oxo)diiron^{IV} core, in which the two iron atoms are antiferromagnetically coupled.[29] The EXAFS study suggested that the coordination number of the iron atoms should be no greater than 5.

One mechanism for the hydroxylation by MMOH is a radical rebound mechanism, which is widely believed to occur in the hydroxylation by cytochrome P450.[10] However, Newcomb, Lippard, and co-workers[30] demonstrated from radical-clock experiments that a measured lifetime of a putative radical species in the MMOH catalysis is

Scheme 4

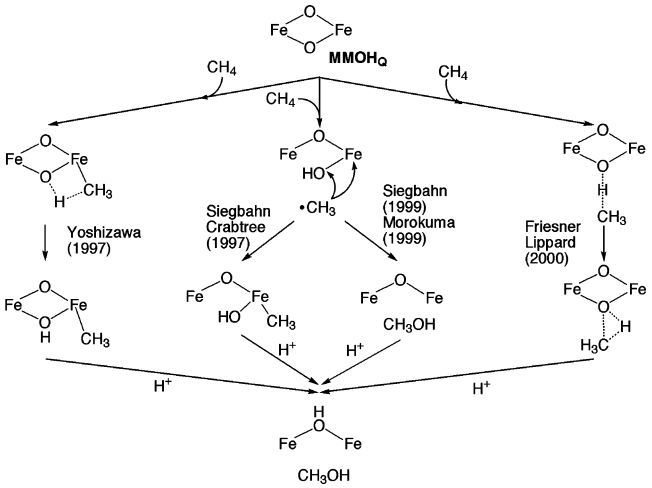

shorter than ~150 fs, which is inconsistent with the formation of a discrete radical species. A short lifetime for a radical species was also observed in the hydroxylation of chiral ethane on MMOH.[31] On the other hand, Lipscomb and co-workers[32] proposed the formation of a radical intermediate in the reaction of methylcubane with MMOH. Despite accumulated experimental findings, the mechanism of the C−H activation of methane in the catalytic function of sMMO remains unclear.

Theoretical calculations gave useful information on the veiled methane hydroxylation by **MMOH$_Q$**.[33−36] Scheme 4 summarizes methane hydroxylation mechanisms proposed so far. As shown at the left of Scheme 4, we proposed that methane should be hydroxylated in a nonradical, two-step mechanism if one of the iron atoms at the active site of **MMOH$_Q$** is coordinatively unsaturated. As discussed earlier in this manuscript, an intermediate with an HO−Fe−CH_3 moiety is involved in the hydroxylation reaction. There are other mechanistic proposals for methane hydroxylation by **MMOH$_Q$**. As shown at the center (left) of Scheme 4, Siegbahn and Crabtree proposed using a five-coordinate iron model with high-spin nonet and undecet states that the methyl radical should recombine with an iron center via a weak Fe−CH_3 bond after the H-atom abstraction.[34a] This mechanism is somewhat similar to ours in that methyl radical is trapped during the reaction. On the other hand, as shown at the center (right), Siegbahn[34c,e] and Morokuma and co-workers[35] proposed that a C−H bond of methane is cleaved in a homolytic manner by six-coordinate diiron model complexes in the high-spin states. After the dissociation of a C−H bond of methane, the resultant methyl radical is shifted to the formed OH group. These authors proposed that **MMOH$_Q$**-mediated hydroxylation should proceed along the radical rebound mechanism. In contrast to the radical mechanism, Friesner, Lippard, and co-workers[36] proposed a nonsynchronous concerted mechanism, as indicated at the right of Scheme 4. Since the C−H activation and the rebound process depend on the coordination sphere and spin state of diiron models adopted, it is important to use an appropriate diiron model of **MMOH$_Q$**.

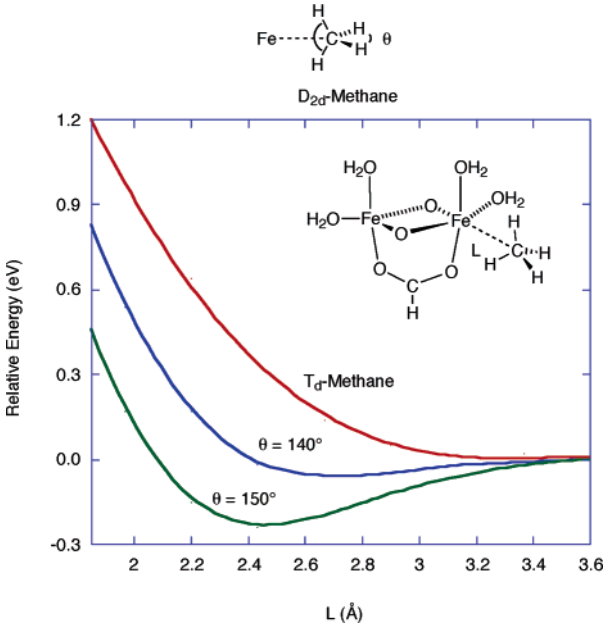

FIGURE 5. Extended Hückel energy diagrams for the coordination of T_d- and D_{2d}-type methanes to a five-coordinate diiron active site of intermediate Q in η^2-binding mode.

In the initial stages of our study on methane activation by sMMO, we tried to look at the interaction between D_{2d}- or C_{3v}-distorted methane and **MMOH$_Q$** using extended Hückel calculations[33a,b] along the lines that Shestakov and Shilov suggested.[37] The total energy diagrams for the coordination of the T_d methane and D_{2d}-distorted methane to a coordinatively unsaturated iron active site are shown in Figure 5. The interaction between D_{2d}-distorted methane and the active site is attractive in this binding mode while that between the T_d methane and the active site is repulsive. A computed binding energy of a D_{2d} methane (with two H−C−H angles opened up to 150°) is about 0.15 eV in this model (at $L = 2.4$ Å), consistent with a calculational result based on a different model with an η^3-binding mode. Methane is thus weakly bound at the five-coordinate iron center of a model of **MMOH$_Q$** both in the η^2-binding mode and in the η^3-binding mode.

Our mechanistic proposals for methane hydroxylation by MMOH are summarized in Figure 6. In contrast to the others, we used the broken-symmetry DFT approach to correctly describe the antiferromagnetic state of the bis-(μ-oxo)diiron^{IV} complex and performed vibrational analyses for the C−H bond cleavage process to characterize the transition state. Since B3LYP calculations showed that the coordinatively unsaturated bis(μ-oxo)diiron^{IV} model of **MMOH$_Q$** lies well below the dissociation limit toward **MMOH$_{red}$** + O_2, such a species can be formed if the release of a water molecule from one of the iron atoms is stabilized in energy by the environmental amino acid residues. The first step in this mechanism is the C−H bond dissociation via **TS1**, and the second step is the recombination of the resultant OH and CH_3 ligands at the active site via **TS2**. The structures of **TS1** and **TS2** are similar to those by the bare FeO^+ complex and the α-oxygen species of Fe-ZSM-5 zeolite.

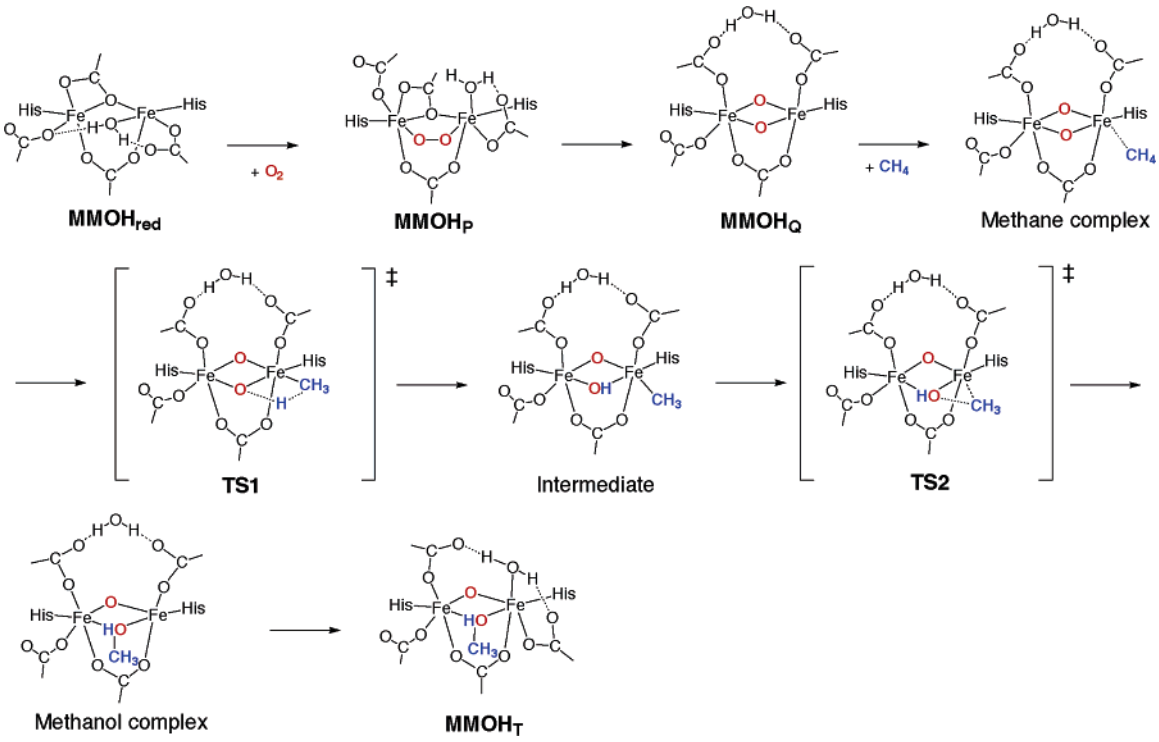

FIGURE 6. Proposed mechanism for dioxygen activation and methane hydroxylation by MMOH.

Table 2. Computed k_H/k_D Values in the H-Atom Abstraction from Methane by MMOH$_Q$ via the Four-Centered Transition State (TS1) in the Broken-Symmetry Singlet State[a]

T (K)	CD_4	CD_3H	CD_2H_2	CDH_3
200	14.8 (25.2)	11.8 (19.7)	9.7 (16.1)	8.3 (13.6)
250	10.8 (17.7)	8.7 (13.9)	7.1 (11.3)	6.0 (9.4)
277	9.5 (15.1)	6.9 (10.7)	6.3 (9.7)	5.3 (8.1)
300	8.6 (13.3)	5.8 (8.5)	5.7 (8.7)	4.8 (7.2)
350	7.1 (10.5)	5.0 (7.1)	4.8 (7.1)	4.1 (5.9)

[a] The values in parentheses include Wigner's tunneling correction.

Let us finally evaluate the nonradical mechanism from the point of view of kinetic isotope effects (KIEs). Lipscomb and co-workers[38] measured from product-distribution analyses after a single turnover KIEs of 4−19 at 277 K; for example, 19 ± 3.9 for 1:1 CH4: CD_4, 12 ± 1 for CD_3H, 9 ± 0.5 for CD_2H_2, and 3.9 ± 1 for CDH_3. Table 2 lists KIEs for the H-atom abstraction via **TS1** computed with transition state theory,[33g] where the values in parentheses include a tunneling correction. As expected, the KIEs significantly decrease with temperature; at 277 K the KIE for the H/D atom abstraction from CH_4/CD_2H_2 is 9.7 after a tunneling correction. This value is in excellent agreement with the value obtained from product distribution analyses at 277 K (9.3 ± 0.5) although this nonradical mechanism is likely to give a small value for KIE.

Concluding Remarks

In this Account we point out that methane hydroxylation can occur in a nonradical, stepwise manner with the bare transition-metal-oxide ions, Fe-ZSM-5 zeolite, and sMMO. The necessity precondition for this mechanism is that the metal-oxo species are coordinatively unsaturated. Direct interaction between methane and the metal active species can form a weakly bound methane complex in the initial stages of these reactions. About 30 years ago, Chatt stated at a certain international conference, "Methane will be the most popular ligand in coordination chemistry".[39] Our proposal is a nice example for his statement. The subsequent C−H bond cleavage to form an intermediate with an HO−Fe−CH_3 moiety and the recombination of the resultant OH and CH_3 ligands take place in a nonradical manner at a metal active site to form a final methanol complex. In this mechanism the methyl radical formed as a result of C−H activation is trapped at the iron site and energetically stabilized. The final ligand coupling we propose from DFT calculations is essentially identical to the mechanism of *Gif* chemistry by Barton.[40] We are now interested in whether this nonradical mechanism can work at the mononuclear and dinuclear copper sites of particulate methane monooxygenase (pMMO).[41]

This work is supported by the Ministry of Culture, Sports, Science and Technology of Japan (MEXT), Japan Society for the Promotion of Science, the Nanotechnology Support Project of MEXT, and CREST of Japan Science and Technology Cooperation.

References

(1) (a) Shilov, A. E. *The Activation of Saturated Hydrocarbons by Transitions Metal Complexes*; Reidel Publishing: Dordrecht, The Netherlands, 1984. (b) Shilov, A. E.; Shul'pin, G. B. Activation of C−H Bonds by Metal Complexes. *Chem. Rev.* **1997**, *97*, 2879−2932.

(2) (a) Crabtree, R. H. *The Organometallic Chemistry of the Transition Metals*; Wiley: New York, 1990. (b) Crabtree, R. H. Aspects of Methane Chemistry. *Chem. Rev.* **1995**, *95*, 987−1007.

(3) (a) Schröder, D.; Schwarz, H. C−H and C−C Bond Activation by Bare Transition-Metal Cations in the Gas Phase. *Angew. Chem., Int. Ed.* **1995**, *34*, 1973−1995. (b) Schwarz, H.; Schröder, D. Concepts of metal-mediated methane functionalization. An intersection of experiment and theory. *Pure Appl. Chem.* **2000**, *72*, 2319−2332.

(4) Arndtsen, B. A.; Bergman, R. G.; Mobley, T. A.; Peterson, T. H. Selective Intermolecular Carbon−Hydrogen Bond Activation by Synthetic Metal Complexes in Homogeneous Solution. *Acc. Chem. Res.* **1995**, *28*, 154−162.

(5) Stahl, S. S.; Labinger, J. A.; Bercaw, J. E. Homogeneous Oxidation of Alkanes by Electrophilic Late Transition Metals. *Angew. Chem., Int. Ed.* **1998**, *37*, 2180−2192.

(6) (a) Feig, A. L.; Lippard, S. J. Reactions of Non-Heme Iron(II) Centers with Dioxygen in Biology and Chemistry. *Chem. Rev.* **1994**, *94*, 759−805. (b) Wallar, B. J.; Lipscomb, J. D. Dioxygen Activation by Enzymes Containing Binuclear Non-Heme Iron Clusters. *Chem. Rev.* **1996**, *96*, 2625−2657. (c) Que, L., Jr.; Dong, Y. Modeling the Oxygen Activation Chemistry of Methane Monooxygenase and Ribonucleotide Reductase. *Acc. Chem. Res.* **1996**, *29*, 190−196. (d) Merkx, M.; Kopp, D. A.; Sazinsky, M. H.; Blazyk, J. L.; Müller, J.; Lippard, S. J. Dioxygen Activation and Methane Hydroxylation by Soluble Methane Monooxygenase: A Tale of Two Irons and Three Proteins. *Angew. Chem., Int. Ed.* **2001**, *40*, 2782−2807.

(7) (a) Schröder, D.; Schwarz, H. FeO^+ activates Methane. *Angew. Chem., Int. Ed. Engl.* **1990**, *29*, 1433−1434. (b) Schröder, D.; Fiedler, A.; Hrusák, J.; Schwarz, H. Experimental and Theoretical Studies toward a Characterization of Conceivable Intermediates Involved in the Gas-Phase Oxidation of Methane by Bare FeO^+. Generation of Four Distinguishable $[Fe, C, H_4, O]^+$ Isomers. *J. Am. Chem. Soc.* **1992**, *114*, 1215−1222.

(8) (a) Anderson, J. R.; Tsai, P. Methanol from Oxidation of Methane by Nitrous Oxide over Fe-ZSM-5 Catalysts. *J. Chem. Soc., Chem. Commun.* **1987**, 1435−1436. (b) Sobolev, V. I.; Dubkov, K. A.; Panna, O. V.; Panov, G. I. Selective Oxidation of Methane to Methanol on an Fe-ZSM-5 Surface. *Catal. Today* **1995**, *24*, 251−252. (c) Dubkov, K. A.; Sobolev, V. I.; Talsi, E. P.; Rodkin, M. A.; Watkins, N. H.; Shteinman, A. A.; Panov, G. I. Kinetic Isotope Effects and Mechanism of Biomimetic Oxidation of Methane and Benzene on Fe-ZSM-5 Zeolite. *J. Mol. Catal. A.: Chemical* **1997**, *123*, 155−161.

(9) Yoshizawa, K. Methane Inversion on Transition Metal Ions: A Possible Mechanism for Stereochemical Scrambling in Metal-Catalyzed Alkane Hydroxylations. *J. Organomet. Chem.* **2001**, *635*, 100−109.

(10) (a) Groves, J. T. Key Elements of the Chemistry of Cytochrome P450. *J. Chem. Educ.* **1985**, *62*, 928−931. (b) Groves, J. T.; Han, Y.-Z. In *Cytochrome P450*, 2nd ed.; Ortiz de Montellano, P. R., Ed.; Plenum: New York, 1995; ch 1.

(11) Chen, Y.-M.; Clemmer, D. E.; Armentrout, P. B. Conversion of CH_4 to CH_3OH: Reactions of CoO^+ with CH_4 and D_2, Co^+ with CH_3OD and D_2O, and $Co^+(CH_3OD)$ with Xe. *J. Am. Chem. Soc.* **1994**, *116*, 7815−7826.

(12) (a) Yoshizawa, K.; Shiota, Y.; Yamabe, T. Reaction Paths for the Conversion of Methane to Methanol Catalyzed by FeO^+. *Chem. Eur. J.* **1997**, *3*, 1160−1169. (b) Yoshizawa, K.; Shiota, Y.; Yamabe, T. Methane-Methanol Conversion by MnO^+, FeO^+, and CoO^+: A Theoretical Study of Catalytic Selectivity. *J. Am. Chem. Soc.* **1998**, *120*, 564−572.

(13) Hall, C.; Perutz, R. N. Transition Metal Alkane Complexes. *Chem. Rev.* **1996**, *96*, 3125−3146.

(14) Yoshizawa, K.; Shiota, Y.; Yamabe, T. Intrinsic Reaction Coordinate Analysis of the Conversion of Methane to Methanol by an Iron-Oxo Species: A Study of Crossing Seams of Potential Energy Surfaces. *J. Chem. Phys.* **1999**, *111*, 538−545.

(15) Shiota, Y.; Yoshizawa, K. A Spin−Orbit Coupling Study on the Spin Inversion Processes in the Direct Methane-to-Methanol Conversion by FeO^+. *J. Chem. Phys.* **2003**, *118*, 5872−5879.

(16) (a) Fiedler, A.; Schröder, D.; Shaik, S.; Schwarz, H. Electronic Structures of Cationic Late-Transition-Metal Oxides. *J. Am. Chem. Soc.* **1994**, *116*, 10734−10741. (b) Shaik, S.; Danovich, D.; Fiedler, A.; Schröder, D.; Schwarz, H. Two-State Reactivity in Organometallic Gas-Phase Ion Chemistry. *Helv. Chim. Acta* **1995**, *78*, 1393−1407. (c) Schröder, D.; Shaik, S.; Schwarz, H. Two-State Reactivity as a New Concept in Organometallic Chemistry. *Acc. Chem. Res.* **2000**, *33*, 139−145.

(17) Shiota, Y.; Yoshizawa, K. Methane to Methanol Conversion by First-Row Transition-Metal Oxide Ions: ScO^+, TiO^+, VO^+, CrO^+, MnO^+, FeO^+, CoO^+, NiO^+, and CuO^+. *J. Am. Chem. Soc.* **2000**, *122*, 12317−12326.

(18) Carter, E. A.; Goddard, W. A., III Early- versus Late-Transition-Metal-Oxo Bonds: The Electronic Structure of VO^+ and RuO^+. *J. Phys. Chem.* **1988**, *92*, 2109−2115.

(19) Centi, G.; Cavani, F.; Trifiró, F. *Selective Oxidation by Heterogeneous Catalysis*; Kluwer: New York, 2001.

(20) (a) Panov, G. I.; Uriarte, A. K.; Rodkin, M. A.; Sobolev, V. I. Generation of active oxygen species on solid surfaces. Opportunity for novel oxidation technologies over zeolite. *Catal. Today* **1998**, *41*, 365−385. (b) Parmon, V. N.; Panov, G. I.; Uriarte, A.; Noskov, A. S. Nitrous oxide in oxidation chemistry and catalysis: application and production. *Catal. Today* **2005**, *100*, 115−131.

(21) (a) Yoshizawa, K.; Yumura, T.; Shiota, Y.; Yamabe, T. Formation of an Iron-Oxo Species upon Decomposition of Dinitrogen Oxide on a Model of Fe-ZSM-5 Zeolite. *Bull. Chem. Soc. Jpn.* **2000**, *73*, 29−36. (b) Yoshizawa, K.; Shiota, Y.; Yumura, T.; Yamabe, T. Direct Methane-Methanol and Benzene-Phenol Conversions on Fe-ZSM-5 Zeolite: Theoretical Predictions on the Reaction Pathways and Energetics. *J. Phys. Chem. B* **2000**, *104*, 734−740.

(22) Heyden, A.; Peters, B.; Bell, A. T.; Keil, F. J. Comprehensive DFT Study of Nitrous Oxide Decomposition over Fe-ZSM-5. *J. Phys. Chem. B* **2005**, *109*, 1857−1873.

(23) Yoshizawa, K.; Shiota, Y.; Kamachi, T. Mechanistic Proposals for Direct Benzene Hydroxylation over Fe-ZSM-5 Zeolite. *J. Phys. Chem. B* **2003**, *107*, 11404−11410.

(24) Yoshizawa, K.; Kagawa, Y. Reaction Pathways for the Oxidation of Methanol to Formaldehyde by an Iron-Oxo Species. *J. Phys. Chem. A* **2000**, *104*, 9347−9355.

(25) Yumura, T.; Amenomori, T.; Kagawa, Y.; Yoshizawa, K. Mechanism for the Formaldehyde to Formic Acid and the Formic Acid to Carbon Dioxide Conversions Mediated by an Iron-Oxo Species. *J. Phys. Chem. A* **2002**, *106*, 621−630.

(26) (a) Rosenzweig, A. C.; Frederick, C. A.; Lippard, S. J.: Nordlund, P. Cryatal structure of a bacterialnonheam iron hydroxylase that catalyses the biological oxidation of methane. *Nature* **1993**, *366*, 537−543. (b) Rosenzweig, A. C.; Nordlund, P.; Takahara, P. M.; Frederick, C. A.; Lippard, S. J. Geometry of the Soluble Methane Monooxygenase Catalytic Diiron Center in Two Oxidation States. *Chem. Biol.* **1995**, *2*, 409−418.

(27) (a) Yoshizawa, K.; Hoffmann, R. Dioxygen Binding to Dinuclear Iron Centers on Methane Monooxygenase Models. *Inorg. Chem.* **1996**, *35*, 2409−2410. (b) Yoshizawa, K.; Yokomichi, Y.; Shiota, Y.; Ohta, T.; Yamabe, T. Density Functional Study on Peroxo Intermediate of Methane Monooxygenase. *Chem. Lett.* **1997**, 587−588. (c) Yumura, T.; Yoshizawa, K. A Vibrational Analysis on Possible Peroxo Forms of Soluble Methane Monooxygenase. *Bull. Chem. Soc. Jpn.* **2004**, *77*, 1305−1311.

(28) Shu, L.; Nesheim, J. C.; Kauffmann, K.; Münck, E.; Lipscomb, J. D.; Que, L. Jr. An $Fe_2^{IV}O_2$ Diamond Core Structure for the Key Intermediate Q of Methane Monooxygenase. *Science* **1997**, *275*, 515−518.

(29) Lee, S.-K.; Fox, B. G.; Froland, W. A.; Lipscomb, J. D.; Münck, E. A Transient Intermediate of the Methane Monooxygenase Catalytic Cycle Containing an $Fe^{IV}Fe^{IV}$ Cluster. *J. Am. Chem. Soc.* **1993**, *115*, 6450−6451.

(30) (a) Liu, K. E.; Johnson, C. C.; Newcomb, M.; Lippard, S. J. Radical Clock Substrate Probes and Kinetic Isotope Effect Studies of the Hydroxylation of Hydrocarbons by Methane Monooxygenase. *J. Am. Chem.* Soc. **1993**, *115*, 939−947. (b) Choi, S.-Y.; Eaton, P. E.; Hollenberg, P. F.; Liu, K. E.; Lippard, S. J.; Newcomb, M.; Putt, D. A.; Upadhyaya, S. P.; Xiong, Y. Regiochemical Variations in Reactions of Methylcubane with *tert*-Butoxyl Radical, Cytochrome P-450 Enzymes, and a Methane Monooxygenase System. *J. Am. Chem. Soc.* **1996**, *118*, 6547−6555.

(31) Valentine, A. M.; Wilkinson, B.; Liu, K. E.; Komar-Panicucci, S.; Priestley, N. D.; Williams, P. G.; Morimoto, H.; Floss, H. G.; Lippard, S. J. Tritiated Chiral Alkanes as Substrates for Soluble Methane Monooxygenase from *Methylococcus capsulatus* (Bath): Probes for the Mechanism of Hydroxylation. *J. Am. Chem. Soc.* **1997**, *119*, 1818−1827.

(32) (a) Jin, Y.; Lipscomb, J. D. Probing the Mechanism of C−H Activation: Oxidation of Methylcubane by Soluble Methane Monooxygenase from *Methylosinus trichosporium* OB3b. *Biochemistry* **1999**, *38*, 6178−6186. (b) Brazeau, B. J.; Austin, R. N.; Tarr, C.; Groves, J. T.; Lipscomb, J. D. Intermediate Q from Soluble Methane Monooxygenase Hydroxylates the Mechanistic Substrate Probe Norcarane: Evidence for a Stepwise Reaction. *J. Am. Chem. Soc.* **2001**, *123*, 11831−11837.

(33) (a) Yoshizawa, K.; Yamabe, T.; Hoffmann, R. Possible Intermediates for the Conversion of Methane to Methanol on Dinuclear Iron Centers of Methane Monooxygenase Models. *New J. Chem.* **1997**, *21*, 151−161. (b) Yoshizawa, K.; Ohta, T.; Yamabe, T.; Hoffmann, R. Dioxygen Cleavage and Methane Activation on Diiron Enzyme Models: A Theoretical Study. *J. Am. Chem. Soc.* **1997**, *119*, 12311−12321. (c) Yoshizawa, K. Two-Step Concerted Mechanism for Alkane Hydroxylation on the Ferryl Active Site of Methane Monooxygenase. *J. Biol. Inorg. Chem.* **1998**, *3*, 318−324. (d) Yoshizawa, K.; Ohta, T.; Yamabe, T. Methane Hydroxylation on a

Diiron Model of Soluble Methane Monooxygenase. *Bull. Chem. Soc. Jpn.* **1998**, *71*, 1899−1909. (e) Yoshizawa, K.; Suzuki, A.; Shiota, Y.; Yamabe, T. Conversion of Methane to Methanol on Diiron and Dicopper Enzyme Models of Methane Monooxygenase: A Theoretical Study on a Concerted Reaction Pathway. *Bull. Chem. Soc. Jpn.* **2000**, *73*, 815−827. (f) Yoshizawa, K. Two-Step Concerted Mechanism for Methane Hydroxylation on the Diiron Active Site of Soluble Methane Monooxygenase. *J. Inorg. Biochem.* **2000**, *78*, 23−34. (g) Yoshizawa, K.; Yumura, T. A Non-Radical Mechanism for Methane Hydroxylation at the Diiron Active Site of Soluble Methane Monooxygenase. *Chem. Eur. J.* **2003**, *9*, 2347−2358.

(34) (a) Siegbahn, P. E. M.; Crabtree, R. H. Mechanism of C−H Activation by Diiron Methane Monooxugenases: Quantum Chemical Studies. *J. Am. Chem. Soc.* **1997**, *119*, 3103−3113. (b) Siegbahn, P. E. M.; Crabtree, R. H.; Nordlund, P. Mechanism of Methane Monooxygenase-A Structural and Quantum Chemical Perspective. *J. Biol. Inorg. Chem.* **1998**, *3*, 314−317. (c) Siegbahn, P. E. M. Theoretical Model Studies of the Iron Dimer Complex of MMO and RNR. *Inorg. Chem.* **1999**, *38*, 2880−2889. (d) Siegbahn, P. E. M.; Blomberg, M. R. A. Transition-Metal Systems in Biochemistry Studied by High-Accuracy Quantum Chemical Methods. *Chem. Rev.* **2000**, *100*, 421−438. (e) Siegbahn, P. E. M. O−O Bond Cleavage and Alkane Hydroxylation in Methane Monooxygenase. *J. Biol. Inorg. Chem.* **2001**, *6*, 27−45.

(35) (a) Basch, H.; Mogi, K.; Musaev, D. G.; Morokuma, K. Mechanism of the Methane-Methanol Conversion Reaction Catalyzed by Methane Monooxygenase: A Density Functional Study. *J. Am. Chem. Soc.* **1999**, *121*, 7249−7256. (b) Basch, H.; Musaev, D. G.; Mogi, K.; Morokuma, K. Theoretical Studies on the Mechanism of the Methane-Methanol Conversion Reaction Catalyzed by Methane Monooxygenase: O−Side vs N−Side Mechanisms. *J. Phys. Chem. A* **2001**, *105*, 3615−3622. (c) Basch, H.; Musaev, D. G.; Morokuma, K. A Density Functional Study of the Completion of the Methane Monooxygenase Catalytic Cycle. Methanol Complex to MMOH Resting State. *J. Phys. Chem. B* **2001**, *105*, 8452−8460. (d) Torrent, M.; Musaev, D. G.; Basch, H.; Morokuma, K. Computational Studies of Reaction Mechanisms of Methane Monooxygenase and Ribonucleotide Reductase. *J. Comput. Chem.* **2002**, *23*, 59−76.

(36) (a) Dunietz, B. D.; Beachy, M. D.; Cao, Y.; Whittington, D. A.; Lippard, S. J.; Friesner, R. A. Large Scale ab Initio Quantum Chemical Calculation of the Intermediates in the Soluble Methane Monooxygenase Catalytic Cycle. *J. Am. Chem. Soc.* **2000**, *122*, 2828−2839. (b) Gherman, B. F.; Dunietz, B. D.; Whittington, D. A.; Lippard, S. J.; Friesner, R. A. Activation of the C−H Bond of Methane by Intermediate Q of Methane Monooxygenase: A Theoretical Study. *J. Am. Chem. Soc.* **2001**, *123*, 3836−3837. (c) Friesner, R. A.; Dunietz, B. D. Large-Scale ab Initio Quantum Chemical Calculations on Biological Systems. *Acc. Chem. Res.* **2001**, *34*, 351−358. (d) Guallar, V.; Gherman, B. F.; Miller, W. H.; Lippard, S. J.; Friesner, R. A. Dynamics of Alkane Hydroxylation at the Non-Heme Diiron Center in Methane Monooxygenase. *J. Am. Chem. Soc.* **2002**, *124*, 3377−3384.

(37) Shestakov, A. F.; Shilov. A. E. Five-Coordinate Carbon Hydroxylation Mechanism. *Zh. Obshch. Khim.* **1995**, *65*, 60−67; *J. Mol. Catal. A* **1996**, *105*, 1−7.

(38) Nesheim, J. C.; Lipscomb, J. D. Large Kinetic Isotope Effects in Methane Oxidation Catalyzed by Methane Monooxygenase: Evidence for C−H Bond Cleavage in a Reaction Cycle Intermediate. *Biochemistry* **1996**, *35*, 10240−10247.

(39) Statement at the 17th International Conference on Coordination Chemistry, Hamburg, 1976; see Shilov, A. E. *Metal Complexes in Biomimetic Chemical Reactions*; CRC: Boca Raton 1996, ch 2.

(40) Barton, D. H. R.; Doller, D. The Selective Functionalization of Saturated Hydrocarbons: Gif Chemistry. *Acc. Chem. Res.* **1992**, *25*, 504−512.

(41) Lieberman, R. L.; Rosenzweig, A. C. Crystal structure of a membrane-bound metalloenzyme that catalyzes the biological oxidation of methane. *Nature* **2005**, *434*, 177−182.

AR050194T